Materials Science & Engineering C 108 (2020) 110484

Contents lists available at ScienceDirect

Materials Science & Engineering C

journal homepage: www.elsevier.com/locate/msec

Palm readings: *Manicaria saccifera* palm fibers are biocompatible textiles with low immunogenicity

Bryan D. James[a], William N. Ruddick[a], Shangradhanva E. Vasisth[a], Krista Dulany[a], Soumitra Sulekar[a], Alicia Porras[b], Alejandro Marañon[c], Juan C. Nino[a], Josephine B. Allen[a,*]

[a] Department of Materials Science and Engineering, University of Florida, 100 Rhines Hall, Gainesville, FL 32611, USA
[b] Mechanical Engineering Department, Universidad de los Andes, CR 1 ESTE 19A 40, Bogota 111711, Colombia
[c] Chemical Engineering Department, Universidad de los Andes, CR, 1 ESTE 19A 40, Bogota, 111711, Colombia

ARTICLE INFO

Keywords:
Biotextile
Natural fiber
Plant-based
Biocompatible
Biomaterial
Manicaria saccifera
Tissue engineering

ABSTRACT

Plant-based fibers are a potential alternative to synthetic polymer fibers that can yield enhanced biocompatibility and mechanical properties matching those properties of tissue. Given the unique morphology of the bract of the *Manicaria saccifera* palm, being an interwoven meshwork of fibers, we believe that these fibers with this built-in structure could prove useful as a tissue engineering scaffold material. Thus, we first investigated the fiber's *in vitro* biocompatibility and immunogenicity. We cultured NIH/3T3 mouse fibroblasts, human aortic smooth muscle cells, and human adipose-derived mesenchymal stem cells on the fiber mats, which all readily attached and over 21 days grew to engulf the fibers. Importantly, this was achieved without treating the plant tissue with extracellular matrix proteins or any adhesion ligands. In addition, we measured the gene expression and protein secretion of three target inflammatory cytokines (IL-1β, IL-8, and TNFα) from THP-1 human leukemia monocytes cultured in the presence of the biotextile as an *in vitro* immunological model. After 24 h of culture, gene expression and protein secretion were largely the same as the control, demonstrating the low immunogenicity of *Manicaria saccifera* fibers. We also measured the tensile mechanical properties of the fibers. Individual fibers after processing had a Young's modulus of 9.51 ± 4.38 GPa and a tensile strength of 68.62 ± 27.93 MPa. We investigated the tensile mechanical properties of the fiber mats perpendicular to the fiber axis (transverse loading), which displayed upwards of 100% strain, but with a concession in strength compared to longitudinal loading. Collectively, our *in vitro* assessments point toward *Manicaria saccifera* as a highly biocompatible biotextile, with a range of potential clinical and engineering applications.

1. Introduction

In recent years, natural materials have gained in notoriety for their use in engineering applications as sustainable alternatives [1]. This interest has not eluded tissue engineering, which requires scaffolds with complex architectures, low-cost, and scalability to transition from the benchtop to the clinic. Plant-based materials offer such properties [2]. Like mammalian tissue, plant tissue is composed of hierarchical structures [3]. Of note is the similarity in mammalian and plant vascular architecture. Decellularized *Spinacia oleracea* (spinach) and *Petroselinum crispum* (parsley) leaves have been used as scaffolds to demonstrate perfusion of plant vasculature by mammalian endothelial cells and cardiomyocytes [4]. In a comparable manner, a range of cell types have been cultured on several decellularized plant stems and leaves, showing variable growth rates. Parsley promoted significant cellular growth of human mesenchymal stem cells and human dermal fibroblasts whereas *Bambusoideae* (bamboo) and *Vanilla planifolia* (vanilla) did not [5]. For these studies it was necessary to modify their decellularized plant tissues with mammalian adhesion peptides or proteins, though it has been shown to be unnecessary for cell attachment and growth on McIntosh red apple hypanthium-derived scaffolds [6]. Biocompatibility of natural materials was demonstrated for these apple-based scaffolds with immunocompetent wild-type C57BL/10ScSnJ mice by the gradual reduction of the immune response several weeks after implantation [7]. Recently, Hickey et al. demonstrated improved cell attachment to their apple-based scaffolds by casting extracellular matrix-based hydrogels onto the scaffolds to form composite plant-derived cellulose biomaterials [8]. However, it is unlikely that the bioactivity and low-immunogenicity of decellularized apple will be the same for other plant-based scaffolds as suggested by the minimal growth of human

* Corresponding author at: Department of Materials Science and Engineering, University of Florida, 206 Rhines Hall, PO Box 116400, Gainesville, FL 32611-6400, USA.
E-mail addresses: jallen@mse.ufl.edu, allen@mse.ufl.edu (J.B. Allen).

https://doi.org/10.1016/j.msec.2019.110484
Received 10 August 2019; Received in revised form 20 November 2019; Accepted 20 November 2019
Available online 27 November 2019
0928-4931/

mesenchymal stem cells and human dermal fibroblasts on both bamboo- and vanilla-based scaffolds [5]. Thus, to consider any new plant-based materials, it is necessary to determine biocompatibility to demonstrate its relevance as a scaffold material.

The *Manicaria saccifera* palm, also known as Ubuçu, Tururi, bucu, monkey cap, *etc.* depending on the region, produces a hollow tubular bract consisting of a brown interwoven, fibrous material with interlocked and bifurcating regions making it a fabric-like biological textile, or biotextile [9]. For the palm, the bract structure acts as a sieve to protect it from insects interested in its inflorescence (flower and associated structures) [10]. The fibers forming the bract are ~100 μm in diameter, are perforated by longitudinal stomata, and are composed of ~67% cellulose and ~31% lignin. The fiber's surface ultrastructure consists of longitudinal ridges and silica surface protrusions (5–10 μm in diameter), which when dislodged leave a crater in the fiber's surface. Bulk properties of the palm's fiber mats have been physically and mechanically characterized displaying slight variability in properties depending on where in the palm bract the mats were sourced [9]. Across a palm bract: water absorptivity ranges from ~70–75%, volumetric density ranges from ~0.80–1.07 g/cm^3, longitudinal Young's modulus ranges from ~1.81–2.42 GPa, longitudinal fracture stress ranges from ~55–82 MPa, and longitudinal strain at failure ranges from ~4.97–5.42%. Because of these properties, the fiber mats have been used as reinforcing fibers in poly(lactic acid) matrix composite materials [11,12]. The unique surface structure of the fibers and the beneficial mechanical properties of the fiber mats suggest *Manicaria saccifera* fibers could be a useful contact guiding plant-based material for tissue engineering composites. To this end, it is necessary to evaluate the mechanical properties of individual *Manicaria saccifera* fibers and their biocompatibility to determine their applicability for tissue engineering applications.

Herein we report the physical and mechanical properties of individual *Manicaria saccifera* fibers and their *in vitro* biocompatibility to support attachment, growth, and survival of mammalian cells as well as their inflammatory response by peripheral blood monocytes.

2. Materials & methods

2.1. Materials

Manicaria saccifera bracts were manually collected by a native community in the Chocó region in Colombia and obtained by A. Marañon at Universidad de los Andes in Colombia as previously described [9]. Native *Manicaria saccifera* bracts vary in length, but sleeve strips 60 to 120 cm long can be typically harvested. For cell culture, the fiber mats were washed, and alkali treated as previously reported to strip away lignin and other surface impurities, and improve their wettability [12]. Representative images of the fibers before and after alkali treatment is presented in Fig. 1. For both mechanical and biocompatibility tests, alkali treated *Manicaria saccifera* individual fibers and fiber mats were sterilized by steam autoclaving at 121 °C for 20 min.

2.2. Tensile testing

Although the mechanical properties of *Manicaria saccifera* bracts have been previously reported by us and others, here we focus our work on the mechanical properties of individual fibers both with and without treatment [9,12,13]. In addition, the mechanical properties of the fiber mat in the transverse direction (*i.e.*, perpendicular to fiber axial direction) were also measured primarily because these have not been extensively reported in literature and to gain further insight into the anisotropic behavior of the mat. Samples were tested using a Stable Micro Systems TA.XT Plus Texture Analyzer. Individual fiber samples from untreated, alkali treated, and alkali treated and autoclaved conditions were analyzed. A minimum of 10 samples per condition were measured. Fiber diameters were individually measured with diameters varying between 250 and 350 μm and cut into specimens with average length of 4.56 cm and then weighed to calculate the individual count number as described below. Consistent with previously reported values, 0.97 specific gravity was used for the fibers [14]. To secure the fibers in the tensile testing grips, the fibers were embedded in polydimethylsiloxane elastomer or secured in masking tape. No apparent difference in the load-displacement curves was found between the two methods for securing the fibers. All specimens were tested to failure at strain rates of 0.17 mm/s (10 mm/min). The effective stress was calculated from tenacity and specific gravity of the fibers using $\gamma = F/T_m$ (1) and $\sigma = 10 g_{sp}\gamma$ (2) where γ is tenacity (cN/tex), F is the load (cN), T_m is the count number (tex = g/km), σ is stress (MPa) and g_{sp} is specific gravity [15]. The Young's modulus was estimated from the slope of the initial linear region of each stress-strain curve. Tensile strength was taken as the stress at failure.

2.3. Cell culture

Four different cell types were cultured with the *Manicaria saccifera* fibers, NIH/3T3 (ATCC® CRL1658™) (NIH3T3s), human adipose-derived mesenchymal stem cells (HADSCs) (Lifeline Cell Technologies), human aortic smooth muscle cells (HAoSMCs) (Cell Applications), and THP1 (ATCC® TIB202™). NIH3T3s were cultured in Dulbecco's Modified Eagle Media (Corning) media supplemented with 10% heat-inactivated fetal bovine serum (Corning), 1% penicillin/streptomycin (Corning), and 1% amphotericin-B (Corning). HADSCs were cultured in StemLife MSC complete media (Lifeline Cell Technologies). AoSMCs were cultured in human SMC complete media (Cell Applications). THP-1 monocytes were cultured in RPMI medium 1640 (Gibco and ATCC) supplemented with 10% non-heat inactivated fetal bovine serum (Corning and Gibco), 0.05 mM β-mercaptoethanol (Bio-Rad and Gibco), 1% penicillin/streptomycin (Corning), and 0.02% amphotericin-B (Corning). All cells were cultured in a humidified incubator with 5% CO_2 at 37 °C. In all cases, the media was changed every 2–3 days.

2.4. Cell attachment, viability, proliferation, and tissue formation

Alkali treated and autoclaved *Manicaria saccifera* fiber mats were cut into small samples of ~4 × 4 × 1 mm. These were then placed into individual wells of a 24-well ultra-low attachment well plate (Corning). NIH3T3s, HADSCs, and HAoSMCs were seeded onto the *Manicaria saccifera* in their respective growth media at 50,000 cells/well. After 48 h, the growth media was removed, fibers washed twice with phosphate-buffered saline (PBS) (Corning) to remove unattached cells, and then fresh media was added to each well. The media was changed every 2–3 days. Images were taken over 21 days to qualitatively visualize cellular attachment and proliferation on the *Manicaria saccifera* fiber mats. At 21 days, staining for viable cells bound to the fiber mats was performed using a Pierce LIVE/DEAD™ Viability/Cytotoxicity Kit, for mammalian cells (Invitrogen) following the manufacturer's protocol. In this assay, live cells stain with green fluorescence from the intracellular uptake of calcein AM, while dead and dying cells stain with red fluorescence from binding of ethidium homodimer-1 to exposed nuclear DNA. The cells attached to the *Manicaria saccifera* were then imaged by fluorescence microscopy. All cell culture imaging was conducted using a Nikon TE2000-U inverted phase contrast/epifluorescence microscope. To assess tissue formation and matrix production, a subset of fiber mats cultured with each cell type were histologically stained and sectioned. The fiber mats were dehydrated in graded ethanol, embedded into paraffin blocks, sectioned as 7 μm slices using a Microm HM355S rotary microtome (Thermo Scientific), and mounted onto glass slides. The sections were then deparaffinized, rehydrated, and stained with hematoxylin and eosin to visualize cells bound to *Manicaria saccifera* fiber mats as well as any extracellular collagen. Stained slide sections were imaged using a Nikon TE2000-U inverted microscope. Fiber ultrastructure after cell culture was imaged by scanning electron microscopy (SEM). Samples were prepared by mounting onto microscopy stubs and coating with gold–palladium or carbon to reduce sample charging. Samples were imaged using a PhenomWorld ProX desktop electron microscope (PhenomWorld) at a beam energy of 10–15 kV.

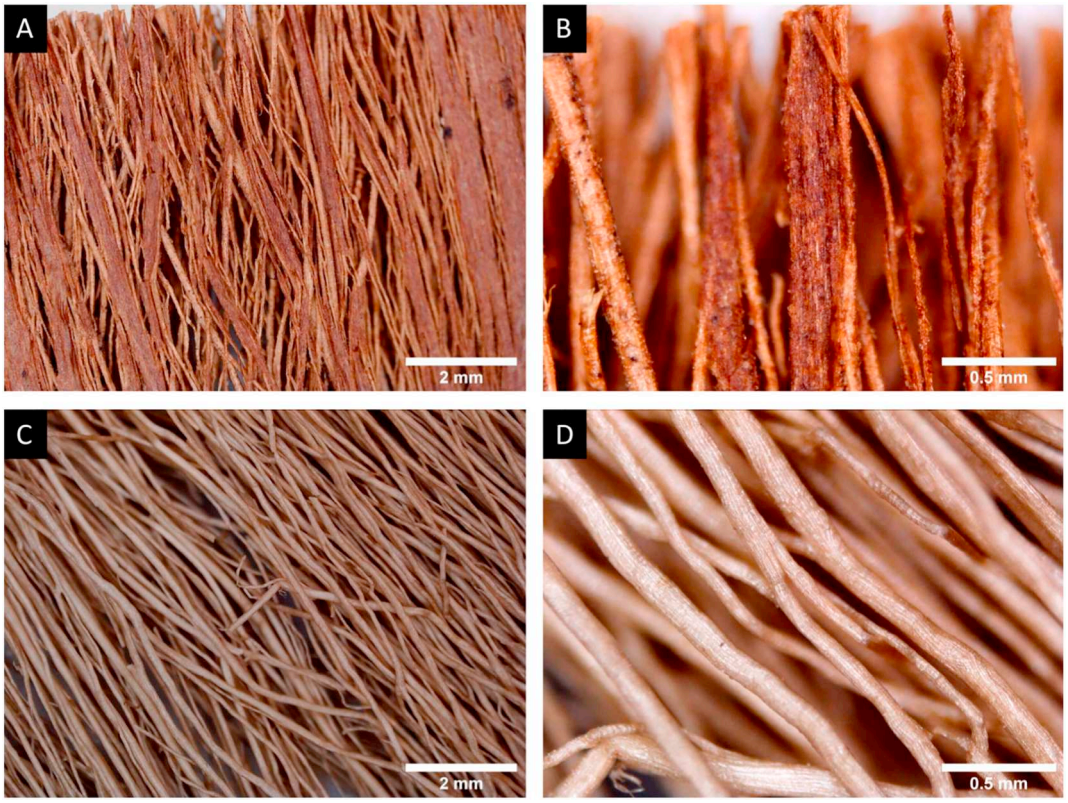

Fig. 1. *Manicaria saccifera* fiber mats before (A, B) and after (C, D) alkali treating. The treatment process is intended to strip away lignin and other surface impurities. Following treatment, the surface of the fibers appeared smoother and fiber color faded.

Table 1
Primer sequences used for THP-1 cell inflammatory gene expression.

Gene	Sequence
Interleukin-1β (IL-1β)	Forward 5′-CAAAGGCGGCCAGGATATAA-3′ Reverse 5′-CTAGGGATTGAGTCCACATTCAG-3′
Interleukin-8 (IL-8)	Forward 5′-AAATCTGGCAACCCTAGTCTG-3′ Reverse 5′-GTGAGGTAAGATGGTGGCTAAT-3′
Tumor necrosis factor-alpha (TNFα)	Forward 5′-GATCCCTGACATCTGGAATCTG-3′ Reverse 5′-GAAACATCTGGAGAGAGGAAGG-3′
β2-microglobulin (B2M)	Forward 5′-CAGCAAGGACTGGTCTTTCTAT-3′ Reverse 5′-ACATGTCTCGATCCCACTTAAC-3′

2.5. In vitro immunogenicity assay

In vitro immunogenicity was assessed by measuring THP-1 monocyte inflammatory gene expression and inflammatory cytokine secretion after culture in the presence of *Manicaria saccifera* fibers. THP-1 cells were seeded at 1,000,000 cells/well into a 24-well ultra-low attachment well plate in their complete growth medium. To assess their inflammatory response to the *Manicaria saccifera* fibers, a sample of the fiber mat (4 × 4 × 1 mm) was added into the well. The addition of 100 μL of PBS and 100 μL of 50 μg/mL lipopolysaccharide (LPS) to separate subcultures were used as negative and positive controls for inflammatory response, respectively. Each condition was measured in triplicate. Following the addition of the materials and reagents, the THP-1 monocytes were incubated for either 4 or 24 h before being collected for gene expression analysis. At 24 h, cell culture media was collected for measuring inflammatory cytokine secretion. The gene expression of three inflammatory cytokine genes in THP-1 monocytes was measured by reverse transcription quantitative polymerase chain reaction (RT-qPCR). Briefly, at 4 and 24 h the THP-1 monocytes were collected and pelleted by centrifugation. Then RNA was isolated and purified for each treatment using a RNeasy Plus Mini Kit (Qiagen) following the manufacturers protocol. Complimentary DNA for each sample was synthesized using an iScript™ cDNA Synthesis Kit (Bio-Rad). RT-qPCR was conducted with a CFX Connect™ Real-Time PCR Detection System (Bio-Rad) using iTaq™ Universal SYBR® Green Supermix (Bio-Rad) and primers from Integrated DNA Technologies for inflammatory cytokine encoding genes (Table 1): interleukin-1β (IL-1β), interleukin-8 (IL-8), tumor necrosis factor-alpha (TNFα), and with housekeeping gene β2-microglobulin (B2M) serving as a reference gene. The ΔΔCq calculation method was used to determine relative gene expression. To assess inflammatory cytokine secretion, after 24 h of culture, aliquots of cell culture media was collected and centrifuged from the different treatments. The relative concentrations of inflammatory cytokines in the supernatant for each sample were determined using a Human Inflammatory Cytokines Multi-Analyte ELISArray™ kit (Qiagen) according to the manufacturer's instructions. The inflammatory cytokines investigated by this array were IL-1β, IL-8, and TNFα.

2.6. Statistical analysis

All statistical analyses were conducted using GraphPad Prism 8. When applicable, student's *t*-test or ANOVA were used to determine statistical significance between conditions using a significance value of 0.05 (Supplementary Table 1). Multiple comparison testing was performed against controls using Dunnett's test and between treatments using Tukey's test. Data is presented as the mean and standard deviation unless otherwise noted.

3. Results

3.1. Manicaria saccifera mechanical properties

Fibers demonstrated a range of tensile behavior by either increasing linearly with increasing strain followed by a slight non-linearity just before failure or following a gradual linear increase with increasing

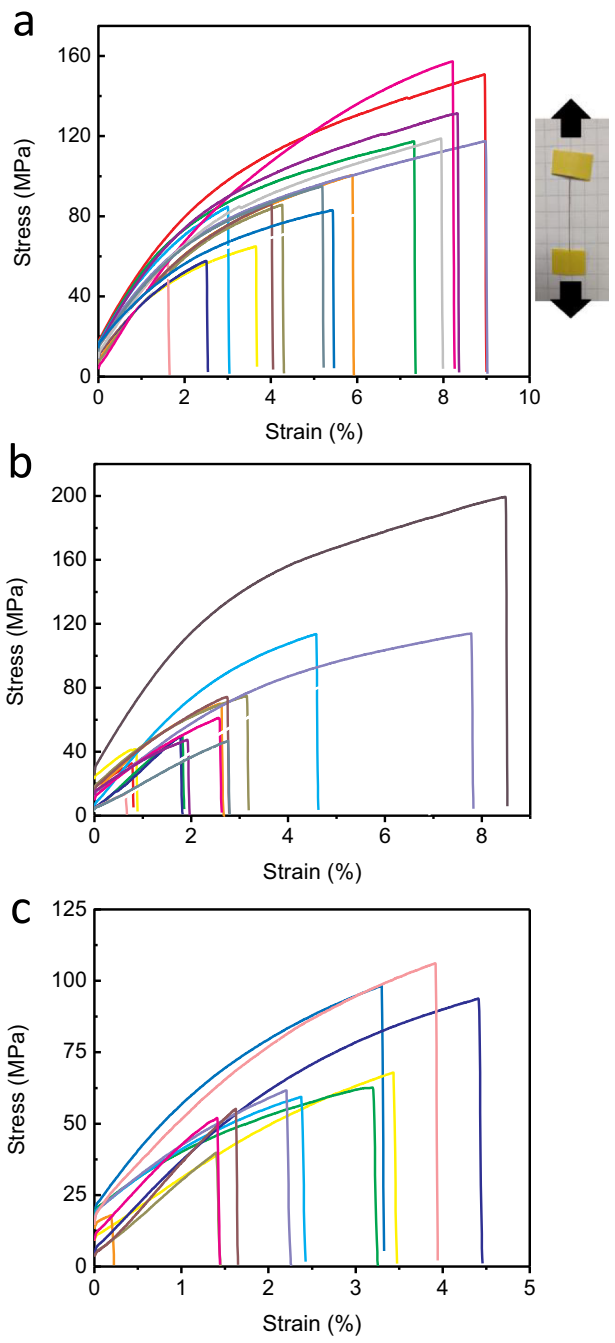

Fig. 2. Individual *Manicaria saccifera* fiber tensile testing: a) untreated fibers, b) alkali treated and c) alkali treated and autoclaved. Fibers were pulled at a strain rate of 10 mm/min (0.17 mm/s). The large degree of variability observed in the stress-strain curves is common in natural fibers.

strain until an inflection point was reached and the stress increased more rapidly with increasing strain until failure. Stress calculated from Equations (1) and (2) was plotted against percent strain (Fig. 2).

Spikes before failure in some curves were attributed to partial failure of the cell columns within the bundles that form each fiber. It is important to note that fiber moduli and strength decreased and strain at failure increased when longer fibers were tested and when fibers were tested at a slower strain rates. Therefore, it is important to compare the results of the mechanical tests on samples with similar lengths and at the same strain rate. Table 2 presents the summary of mechanical properties measured in this work. It is important to note that the alkali and autoclave treatment led to a reduction in the tensile strength and strain at failure with a corresponding increase in the effective Young's modulus. A stiffer fiber after processing, that is also less ductile and less strong is consistent with the anticipated stripping of oils by the alkali treatment and water reduction due to autoclaving.

Previously, the longitudinal mechanical properties of *Manicaria saccifera* fiber mats were reported by our collaborators [9]. With respect to the human body, mechanical loading is not uniform in a single direction and thus, it is necessary to measure the transverse mechanical properties of *Manicaria saccifera* fiber mats. When loaded transversally, the fiber mats were able to sustain significant elongation (> 100% strain) before failure (Fig. 3). This ability was attributed to the fiber mat's lack of cross-weaving in the transverse direction. The transverse Young's modulus was 98 ± 11 Pa and the tensile strength was 12 ± 2 kPa. The fiber mats displayed a trade-off for increased ductility by an accompanied loss in tensile strength. Accordingly, the Young's modulus and tensile strength were found to be much lower than their longitudinal counterpart.

3.2. *Manicaria saccifera* biocompatibility

Over 21 days, cells seeded onto *Manicaria saccifera* fiber mats were imaged. As soon as one day after seeding, cells readily attached to the *Manicaria saccifera* fibers. After 7 days, cell structures were clearly defined as well as cellular organization for all cell types (Fig. 4). The HADSCs appeared to be the least densely organized while HAoSMCs and NIH3T3s grew and engulfed the individual fibers composing the fiber mat. There was significant contact guided alignment of cells along the fiber longitudinal axis. Qualitatively, in all cases, each cell type continued to proliferate through 21 days. In addition, we observed the formation of cellular bridges between proximal fibers, which were at times > 500 μm in distance.

Cell viability after extended culture was assessed using a Pierce™ Live/Dead Viability/Cytotoxicity assay kit. After 21 days, an abundance of cells stained green from the live cell label, calcein AM. Conversely, there was an absence of red ethidium homodimer-1 fluorescence for each cell type indicating there was minimal cell death for cells growing on *Manicaria saccifera* fibers (Fig. 5).

Histological assessments were also conducted to better visualize the interaction between the cells and the fibers. Histological staining revealed and confirmed robust cellular attachment and proliferation onto the *Manicaria saccifera* fibers (Fig. 6). In addition, it further exemplified an observed contact guidance supported by the fibers, which directed cellular alignment several layers thick to be parallel to the fiber longitudinal axis. Multiple layers of cells along with extracellular matrix collagen was seen surrounding the fibers. Interestingly, bridging between individual fibers seen by phase contrast microscopy (Fig. 5) could be viewed histologically (Fig. 6C, D).

Scanning electron microscopy also confirmed cellular attachment for all observed cell types. We observed the robust cellular bridging of

Table 2
Summary of individual *Manicaria saccifera* fiber effective mechanical properties.

Type of fiber	Number of samples	Weight (mg)	Fiber length (cm)	Fiber diameter (μm)	Strain rate (mm/s)	Young's modulus (GPa)	Tensile strength (MPa)	Strain at failure (%)
Untreated	16	1.51 ± 0.25	4.73 ± 0.18	289.31 ± 26.7	0.17	3.10 ± 1.04	99.36 ± 30.45	5.71 ± 2.4
Alkali treated	15	1.09 ± 0.16	4.4 ± 0.46	309.64 ± 45.6	0.17	8.22 ± 4.86	72.38 ± 45.19	3.33 ± 2.52
Alkali treated and autoclaved	11	1.07 ± 0.21	4.56 ± 0.72	310.47 ± 39.55	0.17	9.51 ± 4.38	68.62 ± 27.93	2.80 ± 1.52

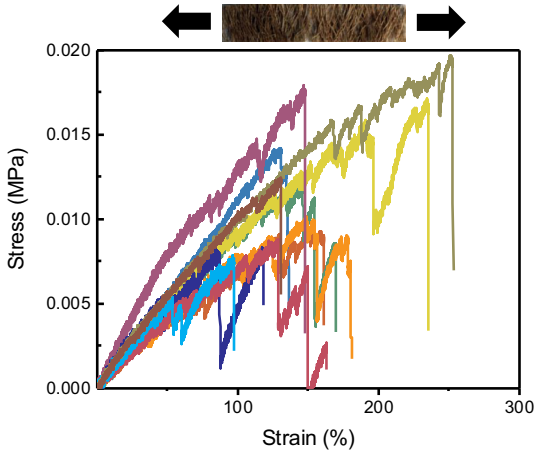

Fig. 3. Transverse tensile loading of *Manicaria saccifera* fiber mats. The fiber mats displayed upwards of 100% strain; however, the mats are significantly weaker compared to longitudinal loading.

NIH3T3s between fibers (Fig. 7A, B). We also saw fiber encapsulation by HADSC (Fig. 7C). In addition, remaining silicate deposits were seen embedded in the circular depressions along the fiber length. (Fig. 7B, D arrows). *Manicaria saccifera* fiber mats promoted contact guided growth and proliferation of mouse fibroblasts, human vascular smooth muscle cells, and human mesenchymal stem cells over an extended period of culture.

3.3. *Manicaria saccifera* immunogenicity

In vitro immunological response was assessed at both the gene and protein expression levels for THP-1 human leukemia monocytes. Gene expression: after 4 h in the presence of *Manicaria saccifera* fiber mats, there was no significant difference in gene expression level for IL-1β, IL-8, or TNFα inflammatory cytokines compared to PBS whereas after 4 h following LPS treatment there was a significant upregulation in gene expression of all three inflammatory cytokines. With LPS treatment at 4 h, IL-1β showed a ~40-fold upregulation while IL-8 and TNFα were upregulated ~20-fold (Fig. 8a). After 24 h in the presence of *Manicaria saccifera* fiber mats, there was a significant upregulation in gene

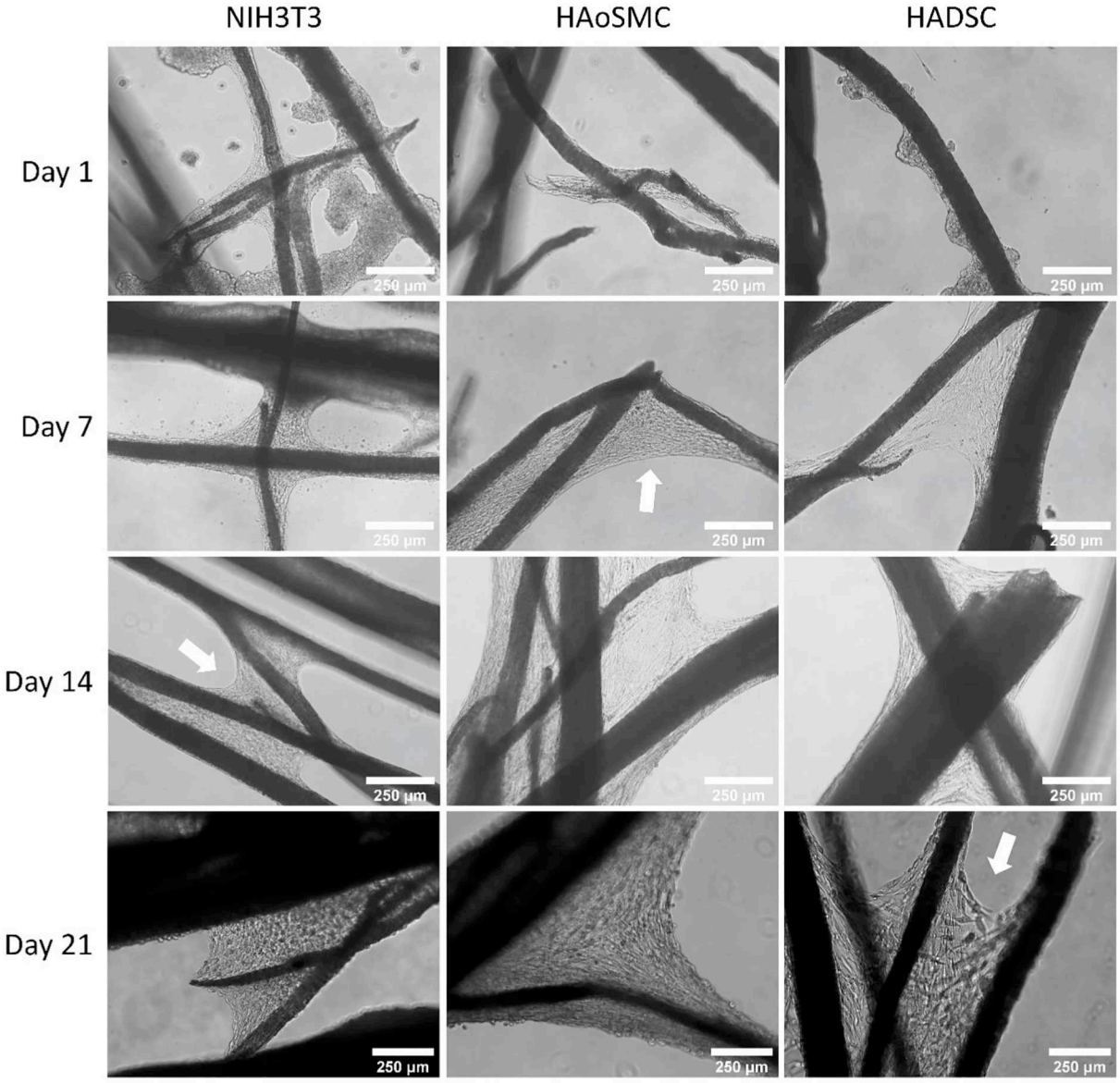

Fig. 4. Extended culture of the different cell types on *Manicaria saccifera* fiber mats. NIH3T3s, HAoSMCs, and HADSCs were all able to attach to the fibers after 1 day. Over a period of 3 weeks, the cells engulfed the fibers and formed webbings between proximal fibers examples of which are indicated by white arrows.

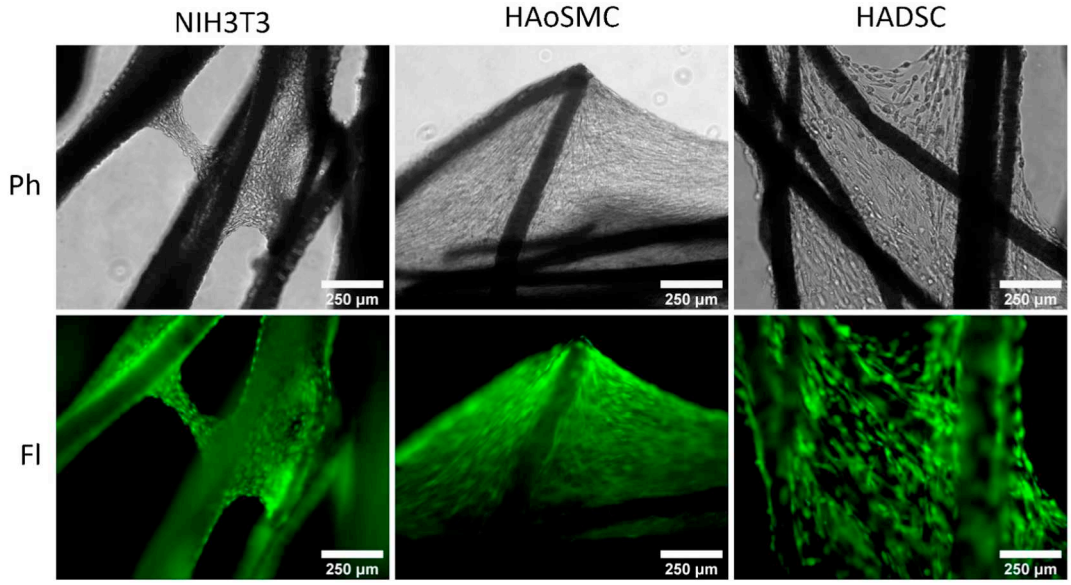

Fig. 5. Cell viability on *Manicaria saccifera* fiber mats. At 21 days, each cell type showed robust cellular viability at multiple levels of thickness indicated by the strong green fluorescence from the calcein AM live cell staining. There were little to no dying or dead cells indicated by the absence of red ethidium homodimer-1 staining in the fluorescence (Fl) images. Phase contrast (Ph) images are shown to indicate the location of the fibers. (For interpretation of the references to color in this figure legend, the reader is referred to the web version of this article.)

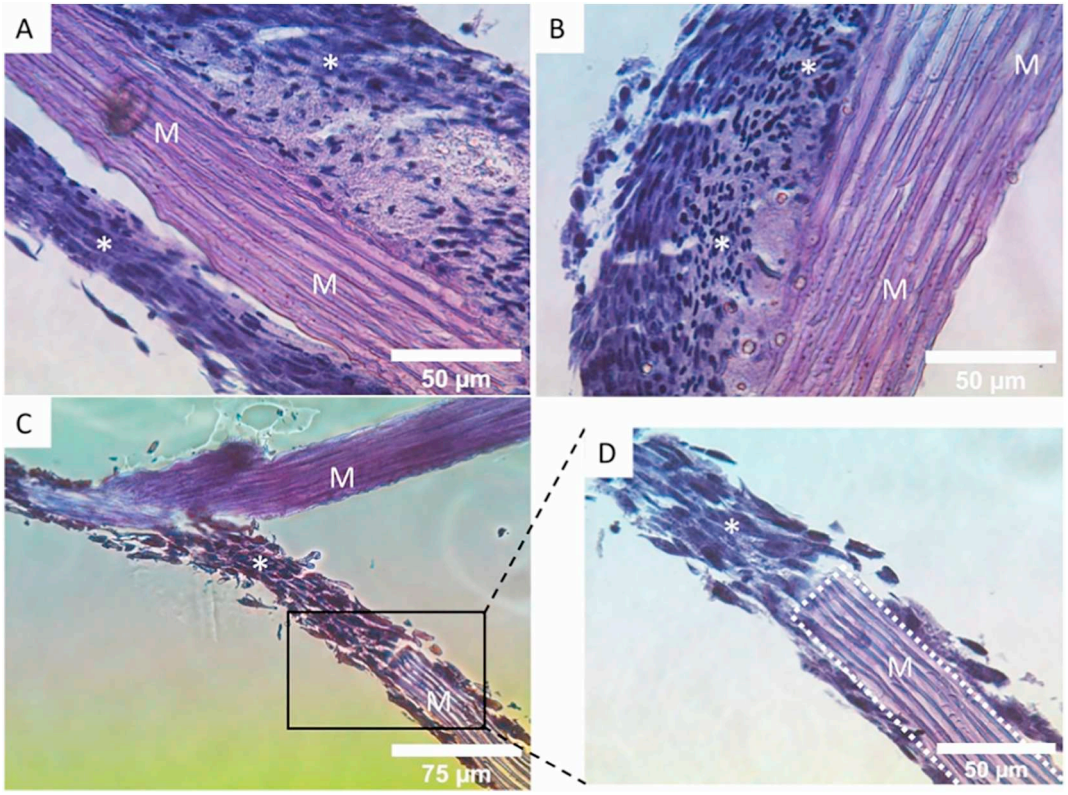

Fig. 6. Histological analysis of NIH/3T3 mouse fibroblasts cultured on *Manicaria saccifera* fiber mats. Sections showed cells aligned along the fiber axis and this alignment extended over several layers of cells (A). Additionally, some regions showed masses of randomly aligned cells surrounded by a layer of several cells aligned with the fiber axis (A, B). Cellular bridging across fibers was also observed (C, D). M = *Manicaria saccifera* fiber, * = NIH/3T3 mouse fibroblasts.

expression only for IL-8 compared to PBS whereas after 24 h following LPS treatment there was no longer significant upregulation in gene expression of TNFα. At 24 h following LPS treatment, IL-1β showed a ~15-fold upregulation, IL-8 showed a ~10-fold upregulation, and TNFα showed a ~5-fold upregulation (Fig. 8b). THP-1 monocytes in the presence of *Manicaria saccifera* fiber mats only showed significant upregulation in IL-8 after 24 h, with a ~5-fold increase (Fig. 8a, b). Protein expression: after 24 h the protein expression agreed well with the gene expression results, realizing the low immunogenicity of *Manicaria saccifera* fibers. There was a statistically significant increase in secretion of every inflammatory cytokine following LPS treatment. After 24 h, THP-1 monocyte secretion of inflammatory cytokines in the

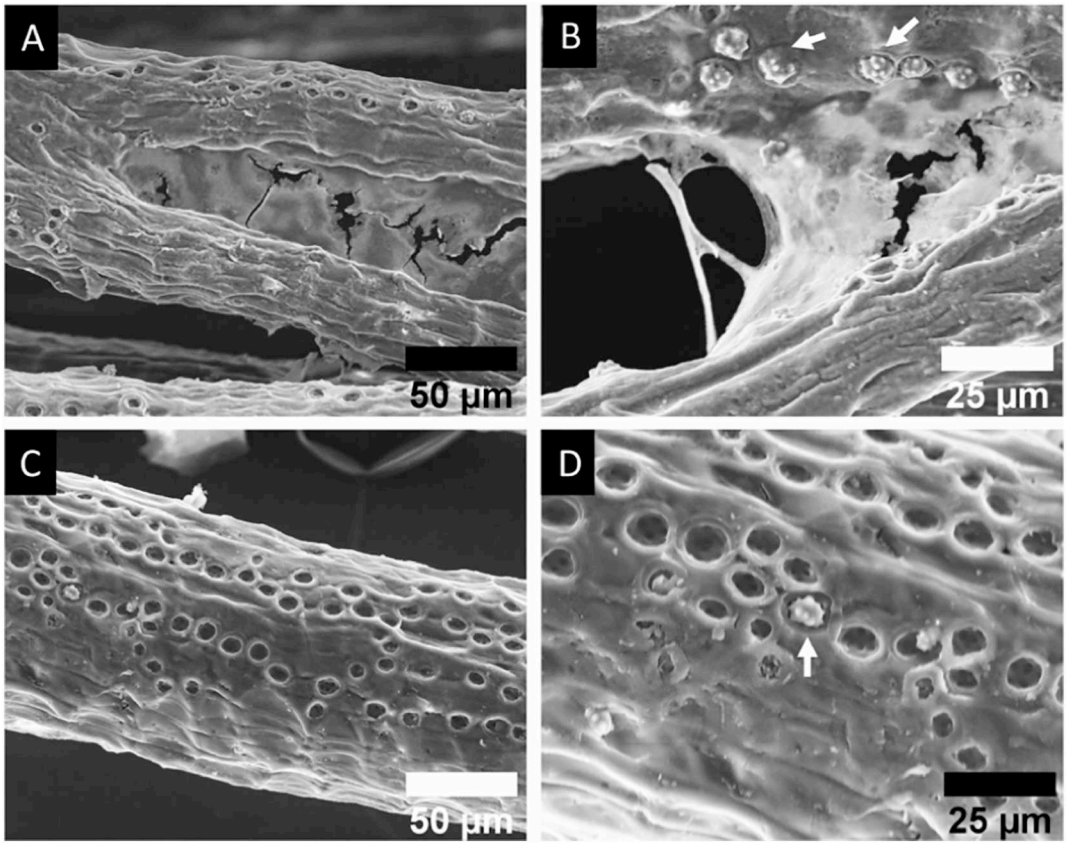

Fig. 7. SEM micrographs of NIH3T3s (A, B) and HADSC (C, D) on *Manicaria saccifera* fibers. Bridging across fibers was observed by SEM (b). Fiber dimples with and without silicate particles were observed marked by arrows (B, D).

presence of *Manicaria saccifera* fiber mats corresponded to a measured absorbance of 0.0017 ± 0.0015 (n = 3) for IL-1β, 0.08 ± 0.03 (n = 3) for IL-8, and 0.011 ± 0.018 (n = 3) for TNFα (Fig. 8c). In comparison, 24 h following LPS treatment corresponded to a measured absorbance of 0.340 ± 0.004 (n = 3) for IL-1β, 3.678 ± 0.009 (n = 2) for IL-8, and 0.42 ± 0.14 (n = 3) for TNFα (Fig. 8c). These values equate to 200 times more IL-1β, 46 times more IL-8, and 38 times more TNFα being secreted after 24 h due to the LPS treatment as compared to the *Manicaria saccifera* fiber mat treatment. Despite a statistically significant difference for secreted IL-1β and IL-8 in the *Manicaria saccifera* treatment as compared to PBS, these values were drastically smaller than those induced by the LPS treatment. From our *in vitro* immunological assessment, we found there was little to no genetic immunological response by THP-1 cells when cultured in the presence of *Manicaria saccifera* fiber mats.

4. Discussion

Our group has identified a promising natural biotextile derived from the Ubuçu palm, *Manicaria saccifera*. The first step to better understand the potential of this material in biological and engineering applications is to demonstrate its *in vitro* biocompatibility. We showed that *Manicaria saccifera* fiber mats promoted mouse fibroblast, human vascular smooth muscle cell, and human adipose-derived mesenchymal stem cell growth over an extended culture period of 21 days. Moreover, these cell types readily attached and encapsulated the fibers without any modification of the fibers by native extracellular matrix proteins. Others have tested the attachment of human mesenchymal stem cells, human dermal fibroblasts, human umbilical vein endothelial cells, human embryonic stem cell derived cardiomyocytes, C2C12 mouse myoblasts, NIH3T3 mouse fibroblasts, HeLa human epithelial cells, and MCF-7 human breast cancer

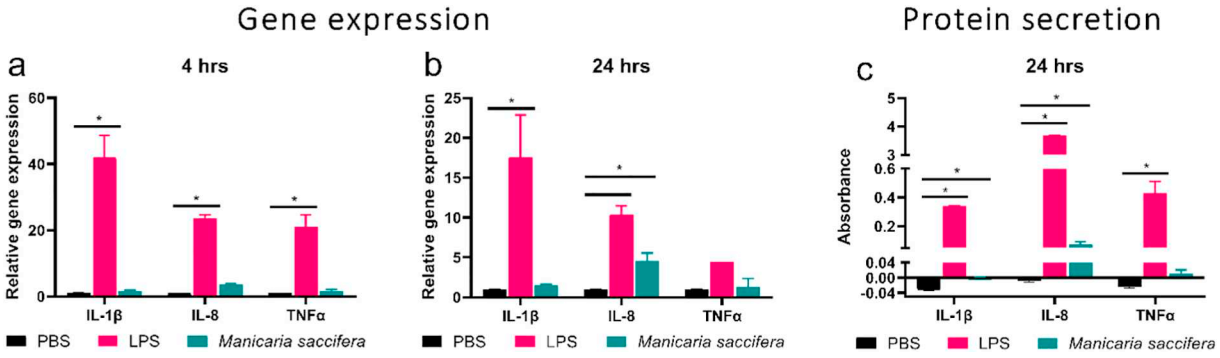

Fig. 8. *In vitro* immunological assessment of *Manicaria saccifera* fiber mats. Gene expression after 4 h (a) and 24 h (b) and protein expression after 24 h (c) of interleukin-1β (IL-1β), interleukin-8, (IL-8), and tumor necrosis factor α (TNFα). Statistical significance between treatments is denoted by *. Treatments were measured in triplicate.

cells to a number of decellularized plants with success only after treating with native extracellular matrix proteins (collagen, gelatin, fibronectin) [4–8,16]. In the case of *Manicaria saccifera*, such treatment was unnecessary for successful cell attachment to the material, which further reduces the amount of processing required for using this biotextile in a biomedical setting. Our fiber mats were only alkali treated and autoclaved prior to cell culture. Alkali treatment of palm fibers has been shown to increase their number of reactive hydroxyl groups [17]. This process likely works to improve cell attachment in the same way that plasma treatment does for polystyrene, which yields a more hydrophilic, negatively charged surface [18]. In a similar manner, NIH3T3 fibroblast growth and attachment to hydrogels produced using agave fibers demonstrated a dependence on sodium hypochlorite treatment conditions [19]. When treated with greater concentrations of sodium hypochlorite, the agave fibers were shown to have diminished lignin and increased hydroxyl group content, as was the case for alkali treated palm fibers. Interestingly, reports of decellularized plant tissue, which used sodium chlorite in their processing required extracellular matrix proteins to promote effective attachment [4,5]. Additionally in the case of decellularized plant tissue, the need to use extracellular matrix proteins to promote effective attachment could be due to remaining lignin following the decellularization treatment whereas an alkali treatment strips the lignin from the fibers [4,5]. Lignin imparts hydrophobicity to cell walls and thus residual lignin at the surface could interfere with cell attachment [5,18,20]. Further chemical analysis of plant tissue after various treatments is required to understand these differences for improving cell attachment to natural materials. This further potentiates the importance of process conditions when treating plant tissue for cell culture. Nonetheless, we show robust cell attachment and proliferation among a variety of divergent cell types.

The attachment data and the near 100% cell viability on the fibers after 21 days of culture support the notion that these fibers are non-cytotoxic. Other studies have shown little to no cytotoxicity for woven natural fibers derived from the ramie plant (*Boehmeria nivea*) and for soy fibers [16,21]. These assessments corroborate our findings that biotextiles pose little cytotoxic effects to cells cultured in their presence; however, neither of these studies showed attachment and growth of cells on these fibers. We observed contact guided cellular alignment with the fiber longitudinal axis, cellular engulfment of the fibers, and cellular bridging between fibers spaced many cell lengths apart. To date, few plant-based materials with intact plant architecture have been investigated for their immunological response. A suture made from woven ramie fibers showed low to mild elevation of IL-1β and TNFα in rats following implantation [16]. Whereas, apple-based cellulose scaffolds also have shown little to no immune response in mice at late time points after implantation [7]. To further demonstrate biocompatibility, we investigated the immunological response of THP-1 human leukemia monocytes cultured in the presence of *Manicaria saccifera* fiber mats. From both gene expression and protein secretion of target inflammatory cytokines, we were able to conclude that the fibers posed little *in vitro* immunogenic response; though, there was a significant upregulation of IL-8 gene expression and elevated protein secretion of IL-8 by THP-1 monocytes after 24 h, which is a proinflammatory cytokine. Future *in vivo* investigations are necessary to elucidate this response as a lasting effect, as other plant-based scaffolds have recovered from an initial severe immune response a few weeks following implantation [7,22]. Collectively, our *in vitro* assessments point toward *Manicaria saccifera* as a highly biocompatible biotextile.

When considering this natural material for biomedical applications, we included investigation of the mechanical properties of both the individual fibers as well as the fiber mat. Previous reports by our collaborators characterized the physical, chemical, and longitudinal tensile properties of *Manicaria saccifera* fiber mats and proposed its use in polymer fiber reinforced composites, which they demonstrated by making a poly-lactic acid composite [9,11,12]. Because the fiber mats have an anisotropic fiber orientation, it was necessary to qualify their transverse mechanical properties. We found that the fiber mats were able to sustain > 100% strain when loaded in the transverse direction; however, the tensile strength was reduced compared to longitudinal loading. Especially, important to biomedical applications are the mechanical properties of the individual fibers because these are the properties sensed at the cellular level [23]. We found that depending on orientation and loading conditions, the fibers are uniquely positioned being stiffer and stronger than common engineering polymers (polyethylene, polyurethane, polymethylmethacrylate, polytetrafluorethylene), while being softer and weaker than other traditional natural fibers (hemp, flax, ramie, cotton) (Fig. 9). Interestingly, both individual fibers and the fiber mat of *Manicaria saccifera* offer elasticity and strength values that are close to that of tendon (Fig. 9). Incorporation of these fibers in a biocompatible composite could prove valuable in achieving modest mechanical property optimization for this target tissue. Importantly, *Manicaria saccifera* fibers are robust and durable. Their mechanical properties showed little change upon alkali treatment and sterilization by autoclaving. These beneficial processing properties and the fibers' extended shelf-life (stored dry at room-temperature indefinitely) further enable their applicability to the clinic where sterilizability and off-the-shelf devices are desired.

Because of its mechanical properties and biocompatibility, a *Manicaria saccifera* biotextile has the potential to be used for many biomedical applications including as, hernia meshes and scaffolds for tendon tissue engineering. Hernia meshes require material properties similar to the abdominal wall (tensile strength ~16 N) and macroporous architecture (pores > 2.5 mm) for tissue in-growth and lower foreign body response [24]. *Manicaria saccifera* mechanical properties fair well (~ 5 N for a single fiber) such that as a composite material these properties can be optimized to match those of the abdominal wall. Given the built-in interwoven meshwork of the fiber mats and its biocompatibility suggest its usefulness as a hernia mesh. Likewise, tendon tissue engineering scaffolds require material properties similar to the native tissue (tensile strength ~50 MPa, Young's modulus ~1.1 GPa), porosity (200–250 μm pores), woven architecture, and biocompatibility [25,26]. *Manicaria saccifera* fibers intrinsically satisfy many of these properties being of comparable tensile strength (~68 MPa) and pore size; though, the fibers are appreciably stiffer (~9×) than native tendon. Especially beneficial is the demonstrated biocompatibility of adipose-derived mesenchymal stem cells on these fibers being a desirable cell source for tissue engineering applications. Given the

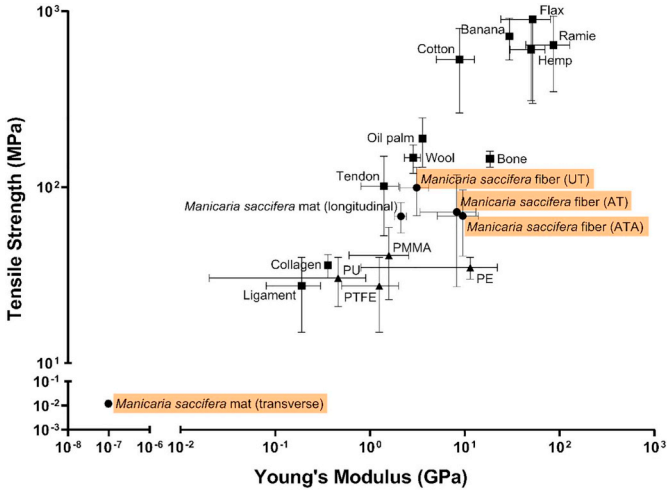

Fig. 9. Ashby plot of natural (■) and common synthetic (▲) materials for tissue engineering. Each material is plotted as a function of the tensile strength and Young's modulus (stiffness). The mechanical properties of Manicaria saccifera individual fibers and fiber mats (●) are highlighted. The transverse fiber mat mechanical properties are shown using a segmented x and y axis in the fig. UT = untreated, AT = alkali treated, ATA = alkali treated and autoclaved, PU = polyurethane, PTFE = polytetrafluoroethylene, PMMA = polymethylmethacrylate, PE = polyethylene. Data compiled was from [9,27–30].

biotextile's mechanical and biocompatible properties, further work is necessary to investigate *Manicaria saccifera* fibers for these promising potential applications.

5. Conclusions

Because of its mechanical properties and biocompatibility, a *Manicaria saccifera* biotextile has the potential to be used for many biomedical applications including as: hernia meshes and scaffolds for tendon tissue engineering. Matching mechanical properties to surrounding tissue is paramount for biomedical devices and thus *Manicaria saccifera* fibers are unique in that they have mechanics remarkably similar to collagenous fibers unlike other natural fibers and engineered plastics [26,28,30–32]. Moreover, these fibers can be easily stored and sterilized by steam autoclaving. Paired with the biotextile's demonstrated *in vitro* biocompatibility, makes it potentially competitive with current hernia mesh and tissue-engineered tendon biomaterials [24,26]. Additionally, *Manicaria saccifera* fiber mats may be used with other materials to form composites further tailoring and expanding the potential applications of this biocompatible biotextile [12]. Plant-based composites are gaining notoriety as next-generation biomaterials and *Manicaria saccifera* promises to expand their utility [27,28].

Funding

This research did not receive any specific grant from funding agencies in the public, commercial, or not-for-profit sectors.

CRediT authorship contribution statement

Bryan D. James:Writing - original draft, Writing - review & editing, Investigation, Formal analysis.**William N. Ruddick**:Investigation, Formal analysis.**Shangradhanva E. Vasisth**:Investigation, Formal analysis.**Krista Dulany**:Investigation.**Soumitra Sulekar**:Investigation, Formal analysis.**Alicia Porras**:Resources.**Alejandro Marañon**:Resources.**Juan C. Nino**:Resources, Conceptualization, Validation, Writing - original draft, Writing - review & editing, Supervision, Project administration.**Josephine B. Allen**:Conceptualization, Validation, Writing - original draft, Writing - review & editing, Supervision, Project administration.

Declaration of competing interest

The authors declare no competing interests.

Appendix A. Supplementary data

Supplementary data to this article can be found online at https://doi.org/10.1016/j.msec.2019.110484.

References

[1] M.I. Misnon, M.M. Islam, J.A. Epaarachchi, K. Lau, Potentiality of utilising natural textile materials for engineering composites applications, Mater. Des. 59 (2014) 359–368, https://doi.org/10.1016/j.matdes.2014.03.022.
[2] U.G.K. Wegst, H. Bai, E. Saiz, A.P. Tomsia, R.O. Ritchie, Bioinspired structural materials, Nat. Mater. 14 (2015) 23–36, https://doi.org/10.1038/nmat4089.
[3] R. Mohammadinejad, S. Karimi, S. Iravani, R.S. Varma, Plant-derived nanostructures: types and applications, Green Chem. 18 (2016) 20–52, https://doi.org/10.1039/C5GC01403D.
[4] J.R. Gershlak, S. Hernandez, G. Fontana, L.R. Perreault, K.J. Hansen, S.A. Larson, B.Y.K. Binder, D.M. Dolivo, T. Yang, T. Dominko, M.W. Rolle, P.J. Weathers, F. Medina-Bolivar, C.L. Cramer, W.L. Murphy, G.R. Gaudette, Crossing kingdoms: using decellularized plants as perfusable tissue engineering scaffolds, Biomaterials 125 (2017) 13–22, https://doi.org/10.1016/j.biomaterials.2017.02.011.
[5] G. Fontana, J. Gershlak, M. Adamski, J.-S. Lee, S. Matsumoto, H.D. Le, B. Binder, J. Wirth, G. Gaudette, W.L. Murphy, Biofunctionalized plants as diverse biomaterials for human cell culture, Adv. Healthc. Mater. 6 (2017) 1601225, , https://doi.org/10.1002/adhm.201601225.
[6] D.J. Modulevsky, C. Lefebvre, K. Haase, Z. Al-Rekabi, A.E. Pelling, Apple derived cellulose scaffolds for 3D mammalian cell culture, PLoS One 9 (2014) e97835, , https://doi.org/10.1371/journal.pone.0097835.
[7] D.J. Modulevsky, C.M. Cuerrier, A.E. Pelling, Biocompatibility of subcutaneously implanted plant-derived cellulose biomaterials, PLoS One 11 (2016) e0157894, , https://doi.org/10.1371/journal.pone.0157894.
[8] R.J. Hickey, D.J. Modulevsky, C.M. Cuerrier, A.E. Pelling, Customizing the shape and microenvironment biochemistry of biocompatible macroscopic plant-derived cellulose scaffolds, ACS Biomater. Sci. Eng. 4 (2018) 3726–3736, https://doi.org/10.1021/acsbiomaterials.8b00178.
[9] A. Porras, A. Maranon, I.A. Ashcroft, Characterization of a novel natural cellulose fabric from Manicaria saccifera palm as possible reinforcement of composite materials, Compos. Part B Eng. 74 (2015) 66–73, https://doi.org/10.1016/j.compositesb.2014.12.033.
[10] J.C. Copete, D.M. Flórez, L.A. Núñez-Avellaneda, Pollination Ecology of the Manicaria saccifera (ARECACEAE): a rare case of pollinator exclusion, Pollinat. Plants, InTech, 2018, , https://doi.org/10.5772/intechopen.76073.
[11] A. Porras, A. Maranon, I.A. Ashcroft, Thermo-mechanical characterization of Manicaria Saccifera natural fabric reinforced poly-lactic acid composite lamina, Compos. Part A Appl. Sci. Manuf. 81 (2016) 105–110, https://doi.org/10.1016/j.compositesa.2015.11.008.
[12] A. Porras, A. Maranon, I.A. Ashcroft, Optimal tensile properties of a Manicaria-based biocomposite by the Taguchi method, Compos. Struct. 140 (2016) 692–701, https://doi.org/10.1016/j.compstruct.2016.01.042.
[13] A.K.F. Oliveira, J.R.M. D'Almeida, Characterization of Ubuçu (Manicaria Saccifera) natural fiber mat, Polym. from Renew. Resour. 5 (2014) 13–28, https://doi.org/10.1177/204124791400500102.
[14] A. Oliveira, J. D'Almeida, Description of the mechanical behavior of different thermoset composites reinforced with Manicaria saccifera fibers, J. Compos. Mater. 48 (2014) 1189–1196, https://doi.org/10.1177/0021998313484622.
[15] E. Kaswell, Wellington Sears Handbook of Industrial Textiles, 1st ed., Wellington Sears Company, Inc, New York, NY, 1963.
[16] R. Kandimalla, S. Kalita, B. Choudhury, D. Devi, D. Kalita, K. Kalita, S. Dash, J. Kotoky, Fiber from ramie plant (Boehmeria nivea): a novel suture biomaterial, Mater. Sci. Eng. C. 62 (2016) 816–822, https://doi.org/10.1016/j.msec.2016.02.040.
[17] A.K.M. Moshiul Alam, M.D.H. Beg, D.M. Reddy Prasad, M.R. Khan, M.F. Mina, Structures and performances of simultaneous ultrasound and alkali treated oil palm empty fruit bunch fiber reinforced poly(lactic acid) composites, Compos. Part A Appl. Sci. Manuf. 43 (2012) 1921–1929, https://doi.org/10.1016/j.compositesa.2012.06.012.
[18] J.A. Ryan, Evolution of cell culture surfaces, BioFiles 3 (8) (2008) 21.
[19] K.L. Tovar-Carrillo, K. Nakasone, S. Sugita, M. Tagaya, T. Kobayashi, Effects of sodium hypochlorite on Agave tequilana Weber bagasse fibers used to elaborate cyto and biocompatible hydrogel films, Mater. Sci. Eng. C. 42 (2014) 808–815, https://doi.org/10.1016/j.msec.2014.06.023.
[20] Q. Liu, L. Luo, L. Zheng, Lignins: biosynthesis and biological functions in plants, Int. J. Mol. Sci. 19 (2018) 335, https://doi.org/10.3390/ijms19020335.
[21] A.T. Wood, D. Everett, K.I. Budhwani, B. Dickinson, V. Thomas, Wet-laid soy fiber reinforced hydrogel scaffold: fabrication, mechano-morphological and cell studies, Mater. Sci. Eng. C. 63 (2016) 308–316, https://doi.org/10.1016/j.msec.2016.02.078.
[22] W.G. Brodbeck, G. Voskerician, N.P. Ziats, Y. Nakayama, T. Matsuda, J.M. Anderson, In vivo leukocyte cytokine mRNA responses to biomaterials are dependent on surface chemistry, J. Biomed. Mater. Res. 64A (2003) 320–329, https://doi.org/10.1002/jbm.a.10425.
[23] J.D. Humphrey, E.R. Dufresne, M.A. Schwartz, Mechanotransduction and extracellular matrix homeostasis, Nat. Rev. Mol. Cell Biol. 15 (2014) 802–812, https://doi.org/10.1038/nrm3896.
[24] S. Bringman, J. Conze, D. Cuccurullo, J. Deprest, K. Junge, B. Klosterhalfen, E. Parra-Davila, B. Ramshaw, V. Schumpelick, Hernia repair: the search for ideal meshes, Hernia 14 (2010) 81–87, https://doi.org/10.1007/s10029-009-0587-x.
[25] C.T. Laurencin, J.W. Freeman, Ligament tissue engineering: an evolutionary materials science approach, Biomaterials 26 (2005) 7530–7536, https://doi.org/10.1016/j.biomaterials.2005.05.073.
[26] N. Yamamoto, K. Ohno, K. Hayashi, H. Kuriyama, K. Yasuda, K. Kaneda, Effects of stress shielding on the mechanical properties of rabbit patellar tendon, J. Biomech. Eng. 115 (1993) 23, https://doi.org/10.1115/1.2895466.
[27] H. Cheung, M. Ho, K. Lau, F. Cardona, D. Hui, Natural fibre-reinforced composites for bioengineering and environmental engineering applications, Compos. Part B Eng. 40 (2009) 655–663, https://doi.org/10.1016/j.compositesb.2009.04.014.
[28] F. Namvar, M. Jawaid, P.M. Tahir, R. Mohamad, S. Azizi, A. Khodavandi, H.S. Rahman, M.D. Nayeri, Potential use of plant fibres and their composites for biomedical applications, BioResources 9 (2014) 5688–5706.
[29] H. Yamada, Strength of Biological Materials, Williams & Wilkins, Baltimore, 1970.
[30] E. Gentleman, A.N. Lay, D.A. Dickerson, E.A. Nauman, G.A. Livesay, K.C. Dee, Mechanical characterization of collagen fibers and scaffolds for tissue engineering, Biomaterials 24 (2003) 3805–3813, https://doi.org/10.1016/S0142-9612(03)00206-0.
[31] A. Goins, A.R. Webb, J.B. Allen, Multi-layer approaches to scaffold-based small diameter vessel engineering: a review, Mater. Sci. Eng. C. 97 (2019) 896–912, https://doi.org/10.1016/j.msec.2018.12.067.
[32] D.R. Sumner, Long-term implant fixation and stress-shielding in total hip replacement, J. Biomech. 48 (2015) 797–800, https://doi.org/10.1016/j.jbiomech.2014.12.021.